



The following Communications have been judged by at least two referees to be “very important papers” and will be published online at [www.angewandte.org](http://www.angewandte.org) soon:

Y. Fu, Q. Dai, W. Zhang, J. Ren, T. Pan,\* C. He\*

**AlkB Domain of Mammalian ABH8 Catalyzes Hydroxylation of 5-Methoxycarbonylmethyluridine at the Wobble Position of tRNA**

M. Roth, P. Kindervater, H.-P. Raich, J. Bargon, H. W. Spiess,\* K. Münnemann\*

**Continuous  $^1\text{H}$  and  $^{13}\text{C}$  Signal Enhancement in NMR Spectroscopy and MRI Using Parahydrogen and Hollow Fiber Membranes**

H. Zheng, J. Gao\*

**Highly Specific Heterodimerization Mediated by Quadrupole Interactions**

M. Willis, M. Götz, A. K. Kandalam, G. F. Ganteför,\* P. Jena\*

**Hyperhalogens: A New Class of Highly Electronegative Species**

V. Mazumder, M. Chi, K. L. More, S. Sun\*

**Synthesis and Characterization of Multimetallic Pd/Au and Pd/Au/FePt Core/Shell Nanoparticles**

S. Scheller, M. Goenrich, S. Mayr, R. K. Thauer, B. Jaun\*

**The Catalytic Cycle of Methyl-Coenzyme M Reductase Proceeds through an Intermediate: Isotope Exchange is Consistent with Formation of a s-Alkane Nickel Complex**

K. P. Neupane, V. L. Pecoraro\*

**Probing a Homoleptic  $\text{PbS}_3$  Coordination Environment in a Designed Peptide Using  $^{207}\text{Pb}$  NMR Spectroscopy: Implications for Understanding the Molecular Basis of Lead Toxicity**

G. Yao, C. Deng,\* X. Zhang, P. Yang

**Efficient Tryptic Proteolysis Accelerated by Laser Radiation for Peptide Mapping in Proteome Analysis**



*“When I was eighteen I wanted to be older and wiser. In ten years time I will be ten years older but probably no wiser ...”*

This and more about Neil Branda can be found on page 7840.

## Author Profile

Neil Branda \_\_\_\_\_ 7840

Chiral Amine Synthesis

Thomas C. Nugent

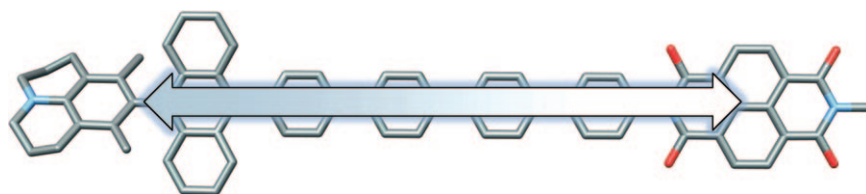
Industrial Biotechnology

Wim Soetaert, Erick J. Vandamme

## Books

reviewed by J. Royer \_\_\_\_\_ 7841

reviewed by R. Stürmer \_\_\_\_\_ 7841



**Getting the message across:** Insight into electronic coupling between electron donors and acceptors connected by molecular bridges (see example) has been achieved by measuring the magnitude of the spin–spin exchange interactions. A

kinetic analysis of the magnetic field effects showed that charge transfer in highly  $\pi$ -conjugated bridges is a function of the spin-selective charge-recombination pathways.

## Highlights

### Molecular Wires

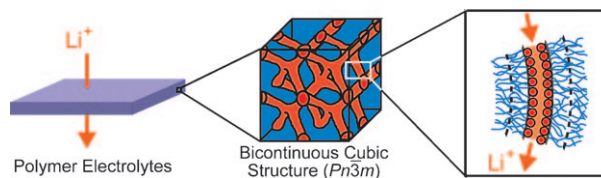
D. M. Guldi\* \_\_\_\_\_ 7844–7846

Putting a Positive Spin on Molecular Bridges

## Liquid Crystals

T. Kato\* — 7847–7848

From Nanostructured Liquid Crystals to  
Polymer-Based Electrolytes



**Self-organized channels:** Molecular assembly of ionic liquid crystals has led to the formation of self-organized 1D, 2D, and 3D ionic channels. Liquid-crystal-based, mechanically stable electrolyte

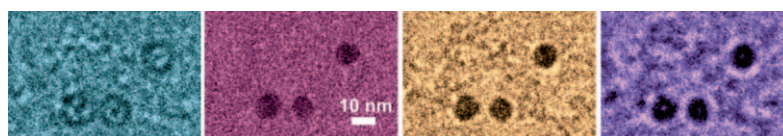
films have been obtained by the formation of a covalent bond network by in situ cross-linking of polymerizable nanostructured ionic liquid crystals (see picture).

## Minireviews

### Nanostructure Analysis

H. Friedrich, P. M. Frederik, G. de With,  
N. A. J. M. Sommerdijk\* — 7850–7858

Imaging of Self-Assembled Structures:  
Interpretation of TEM and Cryo-TEM  
Images



**Get the picture:** Transmission electron microscopy (TEM) is a frequently used analytical method for the direct imaging of solution-borne nanostructures. This Mini-review provides an analysis of the TEM workflow from sample preparation to

acquisition and interpretation of electron micrographs. This should provide a framework for the application of (cryo)-TEM as a powerful and reliable tool for the analysis of colloidal and self-assembled structures with nanoscopic dimensions.

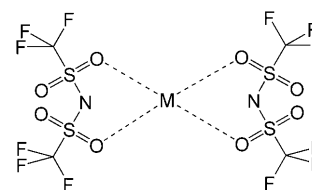
## Reviews

### Homogeneous Catalysis

S. Antonietti, V. Dalla,\*  
E. Duñach\* — 7860–7888

Metal Triflimidates: Better than Metal  
Triflates as Catalysts in Organic  
Synthesis—The Effect of a Highly  
Delocalized Counteranion

**Worth its salt:** The triflimidate anion, by virtue of its highly delocalized charge and steric hindrance, enhances the electrophilic character of the metal center and, therefore, its Lewis acidity. In most cases, triflimidate catalysts are superior to triflates or other salts.



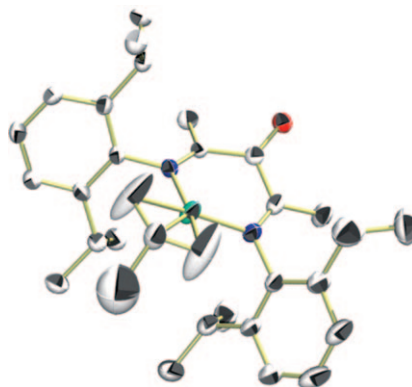
**For the USA and Canada:**  
ANGEWANDTE CHEMIE International  
Edition (ISSN 1433-7851) is published weekly  
by Wiley-VCH, PO Box 191161, 69451 Wein-  
heim, Germany. Air freight and mailing in the  
USA by Publications Expediting Inc., 200  
Meacham Ave., Elmont, NY 11003. Periodicals

postage paid at Jamaica, NY 11431. US POST-  
MASTER: send address changes to *Angewandte  
Chemie*, Journal Customer Services, John  
Wiley & Sons Inc., 350 Main St., Malden,  
MA 02148-5020. Annual subscription price for  
institutions: US\$ 9442/8583 (valid for print and  
electronic / print or electronic delivery); for

individuals who are personal members of a  
national chemical society prices are available  
on request. Postage and handling charges  
included. All prices are subject to local VAT/  
sales tax.

## Communications

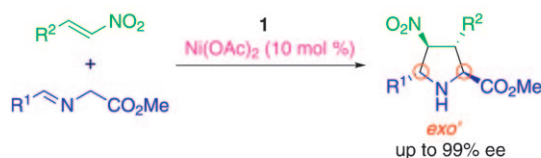
**Complex considerations:** The synthesis and characterization of a discrete cationic nickel–methallyl complex (see structure: Ni green, N blue, O red) provided insight into the propagating sites generated by using  $\alpha$ -keto- $\beta$ -diimine–nickel olefin-polymerization catalysts. The addition of  $\text{Al}(\text{C}_6\text{F}_5)_3$  led to carbonyl coordination to aluminum, further depletion of the electron density at the nickel center, and a substantial increase in reactivity towards ethylene.



### Discrete Cationic Complexes

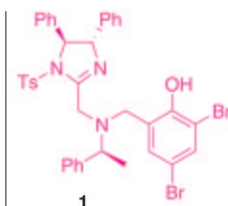
J. D. Azoulay, Z. A. Koretz, G. Wu,  
G. C. Bazan\* 7890 – 7894

Well-Defined Cationic Methallyl  $\alpha$ -Keto- $\beta$ -  
Diimine Complexes of Nickel



**Under control:** A chiral imidazoline–aminophenol/ $\text{Ni}(\text{OAc})_2$  complex promotes the first catalytic asymmetric *exo'*-selective [3+2] cycloaddition of iminoesters and

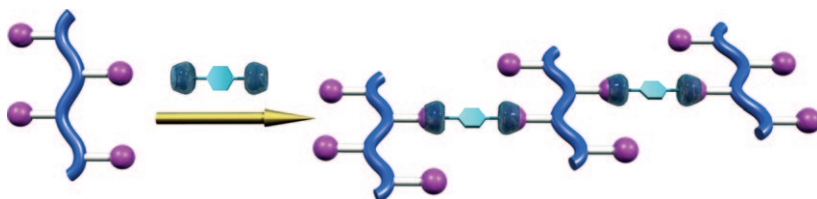
nitroalkenes. Thermodynamic control over the stepwise Michael/Mannich cyclization steps gives the adducts in up to 99% *ee*.



### Cycloaddition

T. Arai,\* N. Yokoyama, A. Mishiro,  
H. Sato 7895 – 7898

Catalytic Asymmetric *exo'*-Selective [3+2]  
Cycloaddition of Iminoesters with  
Nitroalkenes



**Hand in hand:** A polyphenylacetylene with  $\text{C}_{60}$  moieties can be cross-linked by a homoditopic tetrakis(calix[5]arene) host by formation of a specific supramolecular complex (see picture). This noncovalent

interaction leads to an increase of the molecular weight of the polymer and produces morphological changes upon addition of the host.

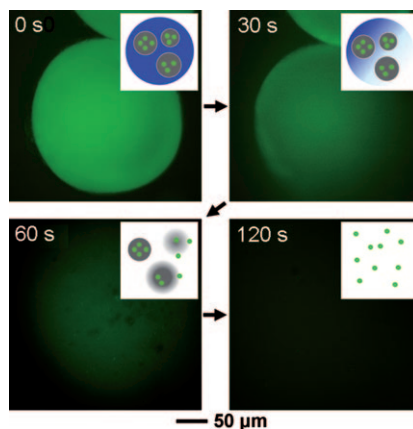
### Supramolecular Cross-Linking

T. Haino,\* E. Hirai, Y. Fujiwara,  
K. Kashiwara 7899 – 7903

Supramolecular Cross-Linking of  
[60]Fullerene-Tagged Polyphenylacetylene  
by the Host–Guest Interaction of  
Calix[5]arene and [60]Fullerene



**Melting away:** Phase-change materials (PCMs) are used to encapsulate colloidal particles with FITC-dextran to demonstrate a new temperature-sensitive drug release system. As the temperature is increased to the melting point of the PCM, the particles leach out, followed by release of FITC-dextran. The initiation and rate of release can be manipulated by using different combinations of materials for the PCM and colloidal particles.



### Drug Release Systems

S. W. Choi, Y. Zhang, Y. Xia\* 7904 – 7908

A Temperature-Sensitive Drug Release  
System Based on Phase-Change Materials



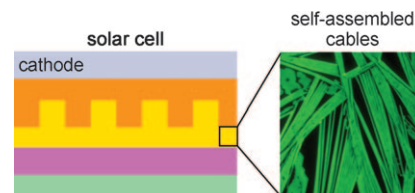
## Molecular Electronics

A. A. Gorodetsky, C.-Y. Chiu, T. Schiros,  
M. Palma, M. Cox, Z. Jia, W. Sattler,  
I. Kymissis, M. Steigerwald,  
C. Nuckolls\* \_\_\_\_\_ **7909–7912**



Reticulated Heterojunctions for  
Photovoltaic Devices

**An organic semiconductor device** is formed by the self-assembly on a transparent electrode surface. The donor (see picture; dibenzotetrathienocoronene, yellow layer) deposits as supramolecular cables, and the acceptor ( $C_{60}$ , orange) subsequently infiltrates this network. This network provides a donor–acceptor interface that is interwoven at the nanoscale. When incorporated into a solar cell, the active layer provides large increases in power conversion efficiencies.



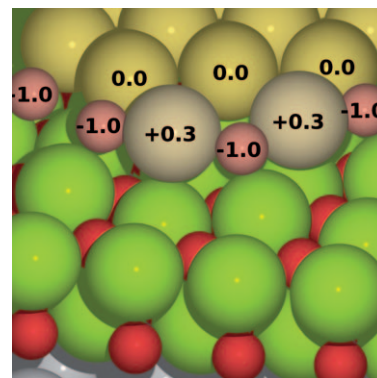
## Gold Clusters

P. Frondelius, H. Häkkinen,\*  
K. Honkala \_\_\_\_\_ **7913–7916**



Formation of Gold(I) Edge Oxide at Flat  
Gold Nanoclusters on an Ultrathin MgO  
Film under Ambient Conditions

**Edgy oxide:** DFT calculations predict the spontaneous formation of a stable one-dimensional edge oxide at the perimeter of a gold cluster on a silver-supported ultrathin MgO film under ambient conditions. The formation of the gold(I) edge oxide is relevant for CO oxidation reactions. Au yellow, gray; Mg green; O red.

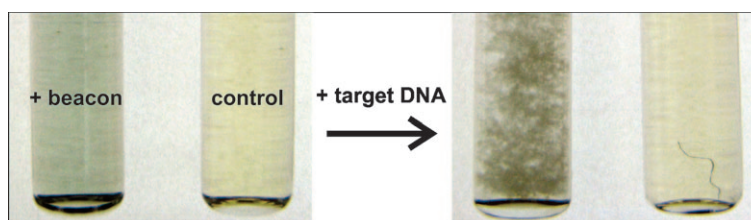


## Nanoparticles

J. F. Lovell, H. Jin, K. K. Ng,  
G. Zheng\* \_\_\_\_\_ **7917–7919**



Programmed Nanoparticle Aggregation  
Using Molecular Beacons



**Out in the open:** Hydrophobically modified molecular beacons were inserted into lipid nanoparticles. Upon addition of the target DNA to a solution of the lipid

nanoparticles, irreversible nanoparticle aggregation occurred (see picture). This aggregation phenomenon results from the opening of the molecular beacons.

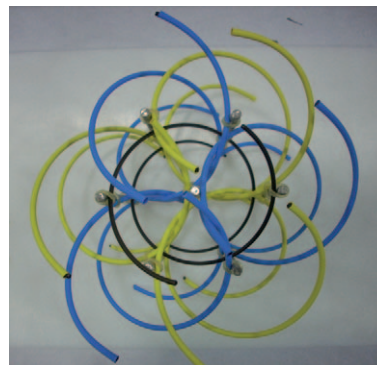
## DNA Structures

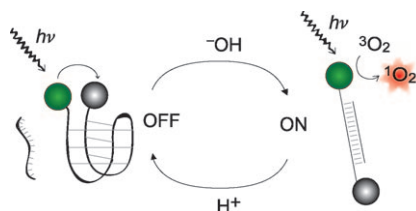
I. Martínez de Ilarduya, D. De Luchi,  
J. A. Subirana, J. L. Campos,\*  
I. Usón\* \_\_\_\_\_ **7920–7922**



A Geometric Approach to the  
Crystallographic Solution of  
Nonconventional DNA Structures:  
Helical Superstructures of d(CGATAT)

**Thinking outside the box:** A geometrical approach for the molecular-replacement solution of DNA crystal structures has been applied to solve the superstructures formed by d(CGATAT). Both B- and Z-form duplexes are stacked and form a complex set of intercrossed helical structures of unique topology.



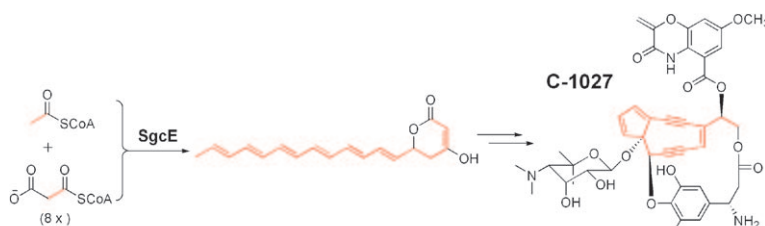


**On again, off again:** Reversible pH-controlled on-and-off switching of a singlet oxygen sensitizer is achieved when an i-motif DNA sequence is employed to control the proximity of a singlet oxygen sensitizer and a quencher (see picture). At pH values less than 5, the i-motif is stable and the singlet oxygen sensitizer quenched, whereas at pH values above 8 the i-motif is denatured and singlet oxygen production is increased by a factor of 35.

### Singlet Oxygen

T. Tørring, R. Toftegaard, J. Arnbjerg, P. R. Ogilby,\* K. V. Gothelf\* **7923–7925**

Reversible pH-Regulated Control of Photosensitized Singlet Oxygen Production Using a DNA i-Motif



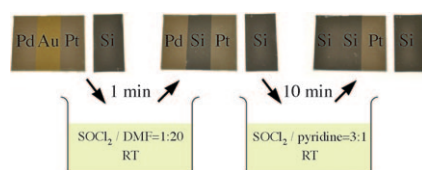
**Not octa- but nonaketide:** The nine-membered enediyne core polyketide synthase SgcE efficiently synthesizes a nonaketide in the absence of any assisting proteins (see scheme), contrary to the

suggestion that an octaketide is the product of the synthase under assistance from a thioesterase. This finding redefines the catalytic functions of the polyketide synthase. CoA = coenzyme A.

### Enediyne Biosynthesis

X. Chen, Z.-F. Guo, P. M. Lai, K. H. Sze,\* Z. Guo\* **7926–7928**

Identification of a Nonaketide Product for the Iterative Polyketide Synthase in Biosynthesis of the Nine-Membered Enediyne C-1027

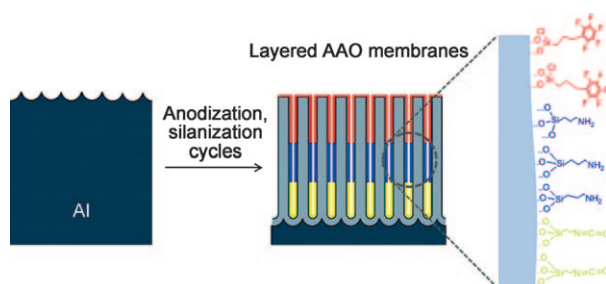


**The noble prize:** Various noble metals can be dissolved in organic solutions with high dissolution rates under mild conditions by using thionyl chloride ( $\text{SOCl}_2$ ) and organic solvents/reagents (pyridine, *N,N*-dimethylformamide, and imidazole). Varying the composition of the solvent and reaction conditions even allows the selective dissolution of noble metals (see picture).

### Solvolysis

W. Lin,\* R. Zhang, S. Jang, C. P. Wong,\* J. Hong **7929–7932**

“Organic Aqua Regia”—Powerful Liquids for Dissolving Noble Metals



**Layers of meaning:** Nanoporous anodic aluminum oxide membranes can be fabricated with multilayered surface functionalities. Membranes produced by this

technique are chemically robust and mechanically stable, and show selectivity towards the transport of small molecules.

### Porous Alumina Membranes

A. M. M. Jani, I. M. Kempson, D. Losic,\* N. H. Voelcker\* **7933–7937**

Dressing in Layers: Layering Surface Functionalities in Nanoporous Aluminum Oxide Membranes





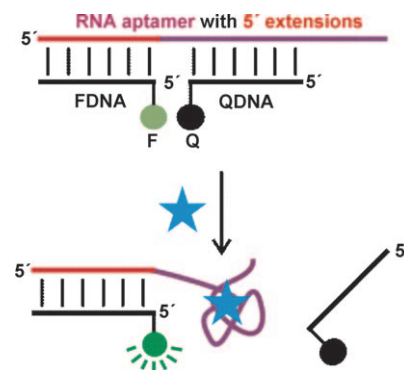
## Biosensors

P. S. Lau, B. K. Coombes,  
Y. Li\* — 7938 – 7942



A General Approach to the Construction of Structure-Switching Reporters from RNA Aptamers

**Three in one:** A three-component, duplex-to-complex structure-switching system is a simple and general strategy for the construction of fluorescent reporters from existing RNA aptamers (see picture). The tagging strategy is attractive as it circumvents the need for the chemical synthesis of modified RNA, and the structure-switching reporters can be used to distinguish targets that have very similar chemical structures.



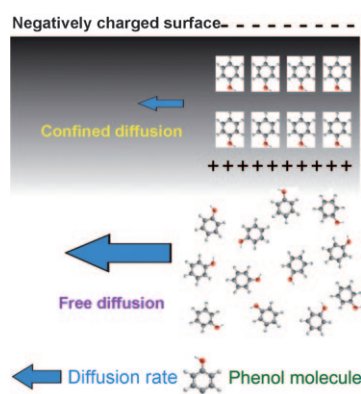
## Diffusion in Nanochannels

W. Chen, Z. Q. Wu, X. H. Xia,\* J. J. Xu,  
H. Y. Chen — 7943 – 7947



Anomalous Diffusion of Electrically Neutral Molecules in Charged Nanochannels

**Confined and free diffusion** of phenol occur in the electric double layer (EDL) and extra-EDL region in the nanochannels of porous anodic alumina (see picture). The inductive effect of the EDL electric field on the phenol molecules slows their diffusion, but it is negligible in the free-diffusion region. The extent of the two regions depends on EDL thickness, and hence the diffusion flux increases with increasing ionic strength of the electrolyte.



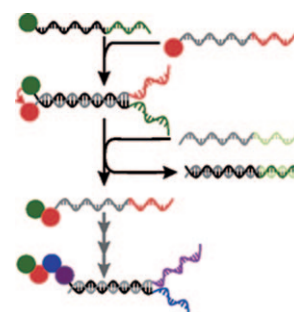
## DNA-Controlled Synthesis

M. L. McKee, P. J. Milnes, J. Bath, E. Stulz,  
A. J. Turberfield,\*  
R. K. O'Reilly\* — 7948 – 7951



Multistep DNA-Templated Reactions for the Synthesis of Functional Sequence Controlled Oligomers

**Biomimetic:** A strand displacement mechanism was designed to permit DNA-templated synthesis of functional oligomers of arbitrary length (see scheme). Key features of the mechanism are that successive coupling reactions take place in near-identical environments and that purification is only necessary in the last synthesis step.



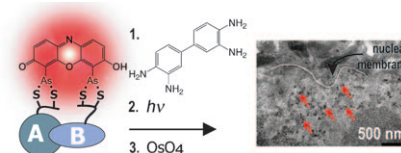
## Protein Imaging

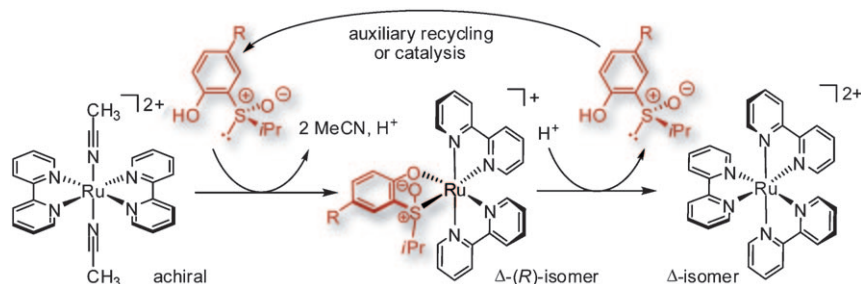
R. J. Dexter, A. Schepartz\* — 7952 – 7954



Direct Visualization of Protein Association in Living Cells with Complex-Edited Electron Microscopy

**Good partnership:** A novel technique called complex-edited electron microscopy (CE-EM) combines bipartite tetra-cysteine display with EM and permits high-resolution imaging of discrete protein complexes (A and B in the picture). The strategy facilitates the direct and selective labeling of discrete protein complexes in living cells, followed by imaging with the extraordinary resolution of EM.





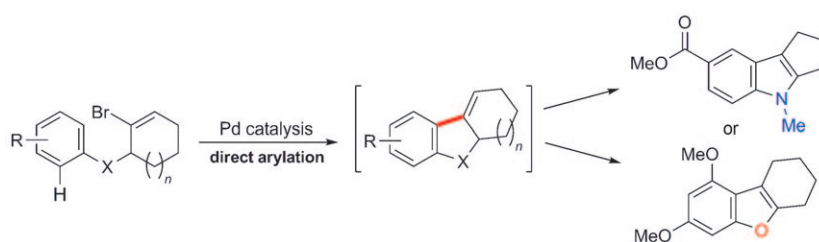
**Asymmetric generator:** Chiral (*S*)-2-(isopropylsulfinyl)phenol and a more electron-rich methoxy derivative ( $R = \text{OCH}_3$ ) are capable of inducing and even catalyz-

ing a chirality-generating *trans*–*cis* isomerization of two 2,2'-bipyridine ligands in an octahedral coordination sphere of a ruthenium complex.

## Asymmetric Catalysis

L. Gong, Z. Lin, K. Harms, E. Meggers\* — 7955 – 7957

Isomerization-Induced Asymmetric Coordination Chemistry: From Auxiliary Control to Asymmetric Catalysis



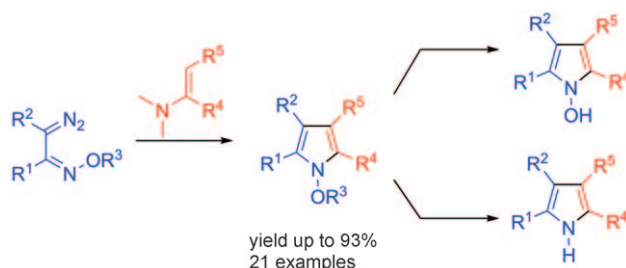
**One route, two cycles:** A palladium-catalyzed intramolecular direct arylation reaction combined with an isomerization step provided a straightforward synthetic route to both indoles and benzofurans (see

scheme). Isolation and functionalization of intermediate alkene isomers allowed the formation of variants having substituents remote from the core.

## Heterocycle Synthesis

M. Yagoubi, A. C. F. Cruz, P. L. Nichols, R. L. Elliott, M. C. Willis\* — 7958 – 7962

Cascade Palladium-Catalyzed Direct Intramolecular Arylation/Alkene Isomerization Sequences: Synthesis of Indoles and Benzofurans



**The stereoselective diazo transfer** reaction with oxime ethers offers an efficient route to the corresponding  $\alpha$ -diazo oxime ethers. The utility of these compounds has

been demonstrated by the synthesis of highly substituted pyrroles through a [3+2] cycloaddition of  $\alpha$ -oximino carbenoids with enamines (see scheme).

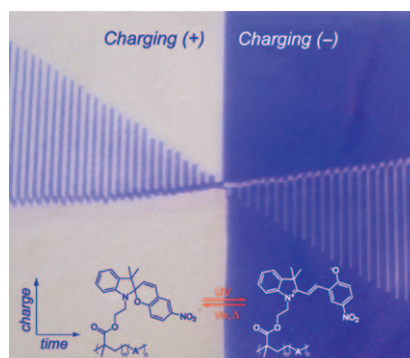
## Cycloaddition

E. Lourdasamy, L. Yao, C.-M. Park\* — 7963 – 7967

Stereoselective Synthesis of  $\alpha$ -Diazo Oxime Ethers and Their Application in the Synthesis of Highly Substituted Pyrroles through a [3+2] Cycloaddition



**Charge switching:** Control of contact electrification was achieved using a combination of photoreactive polymers and light. Upon UV irradiation, polymers substituted with photochromic spiropyrans reversibly switch their rate, and depending on chemical structure, their sign of charging by contact electrification (see picture). Consistent with empirical predictions, these photochromic polymers tended to charge positively upon irradiation with UV light.



## Photochromism

S. Friedle, S. W. Thomas III\* — 7968 – 7971

Controlling Contact Electrification with Photochromic Polymers

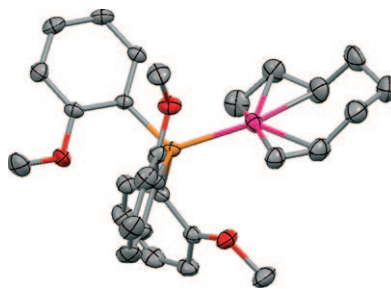


## Nucleophilic Addition

P. J. C. Hausoul, A. N. Parvulescu,  
M. Lutz, A. L. Spek, P. C. A. Bruijninx,  
B. M. Weckhuysen,\*  
R. J. M. Klein Gebbink\* — 7972–7975



Facile Access to Key Reactive  
Intermediates in the Pd/PR<sub>3</sub>-Catalyzed  
Telomerization of 1,3-Butadiene



**Found at last:** A simple and efficient one-pot synthesis procedure leads to several cationic [Pd(1,2,3,7,8-η<sup>5</sup>-octa-2,7-dien-1-yl)(PR<sub>3</sub>)<sub>3</sub>]<sup>+</sup> complexes (see structure; Pd pink, O red, P orange), which are the long sought-after key reactive intermediates in the Pd/PR<sub>3</sub>-catalyzed telomerization of butadiene.



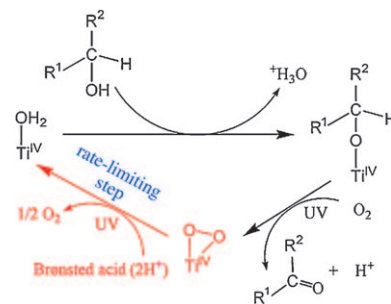
## Heterogeneous Catalysis

Q. Wang, M. Zhang, C. Chen, W. Ma,  
J. Zhao\* — 7976–7979



Photocatalytic Aerobic Oxidation of  
Alcohols on TiO<sub>2</sub>: The Acceleration Effect  
of a Brønsted Acid

**Up to speed:** Brønsted acids adsorbed onto TiO<sub>2</sub> dramatically accelerated the photocatalytic oxidation of alcohols without any loss of selectivity (see scheme). This effect results from the decomposition of the Ti species, having a side-on peroxide, on the TiO<sub>2</sub> surface. The decomposition is aided by the Brønsted acid, thereby regenerating the active Ti sites on the surface of the catalyst.



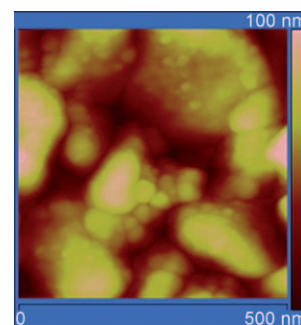
## Plasmon-Induced Enhancement

R. Solarzka, A. Królikowska,  
J. Augustyński\* — 7980–7983



Silver Nanoparticle Induced Photocurrent  
Enhancement at WO<sub>3</sub> Photoanodes

**Silver screen:** Thin silver nanoparticle layers embedded within a 1 μm thick semiconducting WO<sub>3</sub> film on conducting glass substrates enhance optical absorption over a broad wavelength region. The combination of light scattering and nearby electromagnetic-field effects causes a large increase of photocurrents associated with water splitting generated at the WO<sub>3</sub> photoanodes under simulated solar light irradiation.



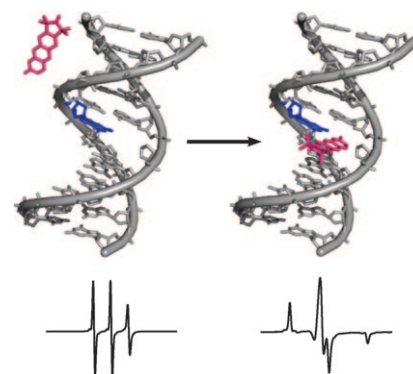
## Noncovalent Spin Labeling

S. A. Shelke,  
S. Th. Sigurdsson\* — 7984–7986



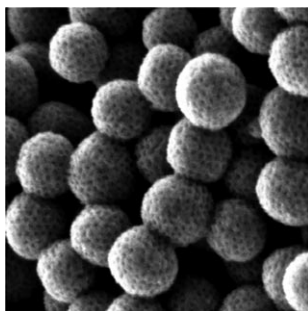
Noncovalent and Site-Directed Spin  
Labeling of Nucleic Acids

**Spin label parking:** The rigid spin label **ζ** (magenta), which is an analogue of cytidine, binds site-specifically to abasic sites in duplex DNAs, through hydrogen bonding to guanine (blue) and π stacking with the flanking base pairs. EPR spectroscopy shows complete binding of **ζ** to the abasic site at low temperatures. This new spin-labeling strategy gives easy access to spin-labeled nucleic acids for structural studies by pulsed EPR techniques.





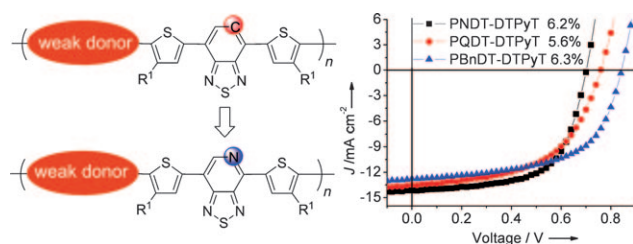
**Mesoporous carbon nanoparticles** with uniform spherical morphology were fabricated through a low-concentration hydrothermal synthesis route. The diameters can be tuned from 20 to 140 nm by varying the reagent concentration. The highly ordered mesoporous carbon nanospheres with high surface area and large pore volume show low cytotoxicity and can easily penetrate into living cells.



## Mesoporous Materials

Y. Fang, D. Gu, Y. Zou, Z. X. Wu, F. Y. Li, R. C. Che, Y. H. Deng, B. Tu, D. Y. Zhao\* 7987–7991

A Low-Concentration Hydrothermal Synthesis of Biocompatible Ordered Mesoporous Carbon Nanospheres with Tunable and Uniform Size



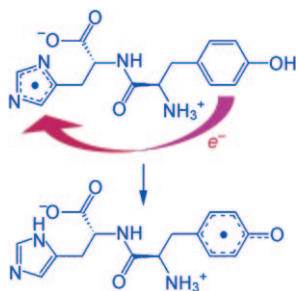
**Mind the gap!** Polymers synthesized by replacing the benzene unit in the acceptor 4,7-dithien-2-yl-2,1,3-benzothiadiazole (DTBT) with a  $\pi$ -electron-deficient pyridine unit (DTPyT) show a smaller bandgap than their DTBT counterparts.

Power conversion efficiencies of over 6% are demonstrated in solar cell studies (see picture; PNDT, PQDT, and PBnDT represent dithiophene derivatives as weak donors).

## Solar Cells

H. Zhou, L. Yang, S. C. Price, K. J. Knight, W. You\* 7992–7995

Enhanced Photovoltaic Performance of Low-Bandgap Polymers with Deep LUMO Levels

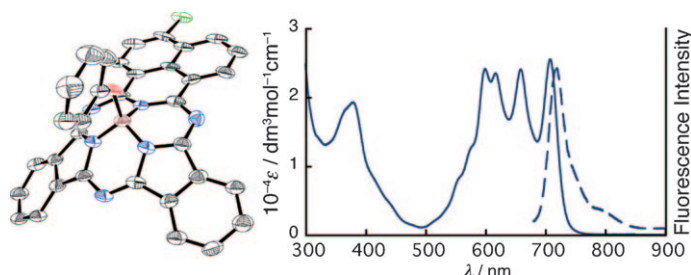


**Invisible to other methods,** reactions of the histidyl radical could be followed by NMR spectroscopic detection of the histidine signal through the use of time-resolved chemically induced dynamic nuclear polarization (CIDNP). CIDNP decay of the His signal during photo-oxidation of the peptides His-Tyr and Tyr-His pointed to electron transfer from the tyrosine residue to the histidyl radical (see scheme for Tyr-His).

## Electron Transfer in Dipeptides

O. B. Morozova, A. V. Yurkovskaya\* 7996–7999

Intramolecular Electron Transfer in the Photooxidized Peptides Tyrosine–Histidine and Histidine–Tyrosine: A Time-Resolved CIDNP Study



**At the core:** A novel core-modified subphthalocyanine analogue has been synthesized (see structure; Cl green, red O, blue N). This molecule comprises a six-membered ring unit in place of a five-

membered ring unit and exhibits unique spectroscopic (see plot) and electrochemical properties originating from the azaphenylene-containing  $14\pi$ -electron conjugation system.

## Subphthalocyanines

H. Zhu, S. Shimizu, N. Kobayashi\* 8000–8003

Subazaphenalenephthalocyanine: A Subphthalocyanine Analogue Bearing a Six-Membered Ring Unit

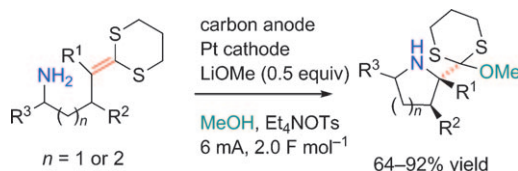


## Anodic Cyclization

H.-C. Xu, K. D. Moeller\* — 8004–8007



Intramolecular Anodic Olefin Coupling Reactions: Use of the Reaction Rate To Control Substrate/Product Selectivity



**Look out—it's a trap!** The anodic coupling of olefins with amine trapping groups to form proline and pipecolic acid derivatives with a quaternary  $\alpha$  carbon atom (see scheme) was successful despite the significantly lower oxidation potential of

the product relative to that of either functional group in the substrate: owing to the very fast cyclization, the oxidation potential of the substrate is lower than that of the product. Ts = *p*-toluenesulfonyl.

## Vanadium Azides

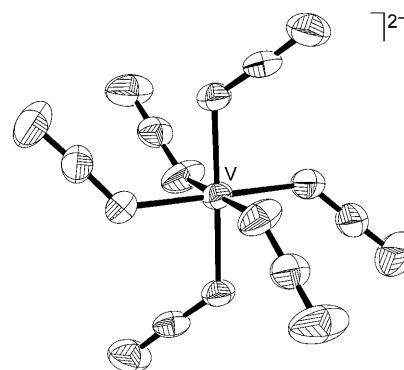
R. Haiges,\* J. A. Boatz,  
K. O. Christie\* — 8008–8012



The Syntheses and Structure of the Vanadium(IV) and Vanadium(V) Binary Azides  $V(N_3)_4$ ,  $[V(N_3)_6]^{2-}$ , and  $[V(N_3)_6]^-$

### Shock-sensitive and highly explosive

$V(N_3)_4$  was prepared from  $VF_4$  and  $Me_3SiN_3$  by fluoride–azide exchange. Salts of the  $[V(N_3)_6]^{2-}$  anion (see picture) were obtained by treatment of the neutral tetraazide with ionic azides. Vanadium(V) azide, the only binary vanadium(V) compound known apart from  $VF_5$ ,  $VF_6^-$ , and  $V_2O_5$ , was successfully prepared from the  $VF_6^-$  anion.

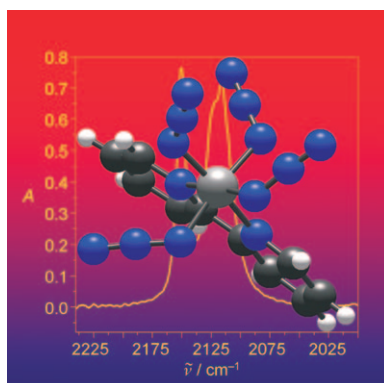


## Silicon Azides

P. Portius,\* A. C. Filippou,\*  
G. Schnakenburg, M. Davis,  
K.-D. Wehrstedt — 8013–8016



Neutral Lewis Base Adducts of Silicon Tetraazide



**Highly energetic and still stable:** The first base adducts of silicon tetraazide,  $Si(N_3)_4(L_2)$  ( $L_2$  = bipyridine, 1,10-phenanthroline), were prepared and fully characterized (picture: the ball and stick model of the adduct with  $L_2$  = 2,2'-bipyridine in front of its FTIR spectrum; dark gray C, white H, light gray Si, blue N). The highly energetic compounds combine a remarkable thermal stability, with a high reactive nitrogen content (up to 48%) and convenient accessibility.

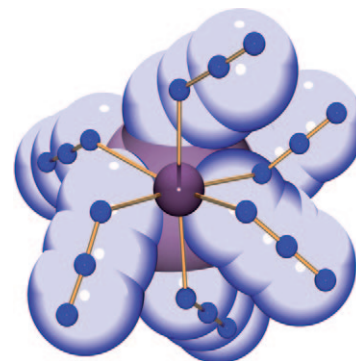
## Bismuth Azides

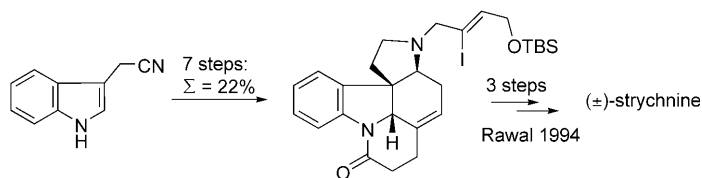
A. Villinger,\* A. Schulz\* — 8017–8020



Binary Bismuth(III) Azides:  $Bi(N_3)_3$ ,  $[Bi(N_3)_4]^-$ , and  $[Bi(N_3)_6]^{3-}$

**Nitrogen finally meets bismuth:** The synthesis of binary bismuth(III) azides  $Bi(N_3)_3$ ,  $[Bi(N_3)_4]^-$ , and  $[Bi(N_3)_6]^{3-}$  along with their characterization is presented for the first time and closes a chapter in main group chemistry.  $Bi(N_3)_3 \cdot THF$  qualifies as a good precursor for the generation of binary BiN owing to its low shock and heat sensitivity, in contrast to pure, highly sensitive  $Bi(N_3)_3$ .





**Brevity is the soul of wit!** The power of  $\text{SmI}_2$ -induced cyclizations has been demonstrated by the shortest formal total synthesis of (±)-strychnine to date, which features a new cascade reaction. Only one

protective-group transformation is required. The ketyl-aryl coupling/acylation cascade also efficiently proceeds with other indole derivatives with excellent diastereoselectivities.

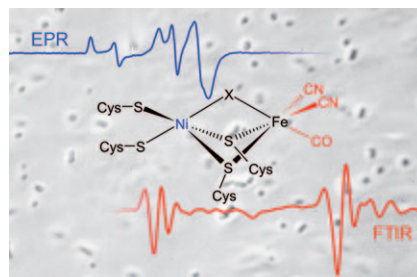
## Natural Products

C. Beemelmans,  
H.-U. Reissig\* ——— 8021–8025

A Short Formal Total Synthesis of Strychnine with a Samarium Diiodide Induced Cascade Reaction as the Key Step



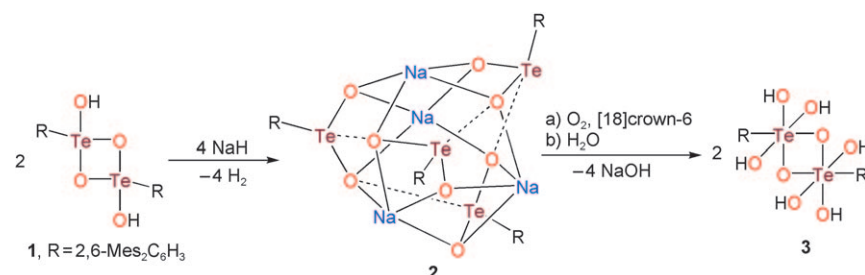
**A clear picture:** In situ EPR and FTIR spectroscopic studies on the soluble,  $\text{NAD}^+$ -reducing  $[\text{NiFe}]$ -hydrogenase of *Ralstonia eutropha* reveal that the catalytic site resides predominantly in the intermediate  $\text{Ni}_a\text{-C}$  state within whole cells. This state, can either be reversibly oxidized to a “ $\text{Ni}_a\text{-B}$ ”-like state or further reduced to various  $\text{Ni}_a\text{-SR}$  species. The data suggest that the iron center in the active site contains a standard set (one CO and two  $\text{CN}^-$ ) of inorganic ligands.



## Biocatalysis

M. Horch, L. Lauterbach, M. Saggu,  
P. Hildebrandt, F. Lenzian, R. Bittl,  
O. Lenz,\* I. Zebger\* ——— 8026–8029

Probing the Active Site of an  $\text{O}_2$ -Tolerant  $\text{NAD}^+$ -Reducing  $[\text{NiFe}]$ -Hydrogenase from *Ralstonia eutropha* H16 by In Situ EPR and FTIR Spectroscopy



**Two for Te:** The ditelluronic acid **3** is the first heavy congener of sulfonic and selenonic acids and is obtained by the  $\text{O}_2$  oxidation of the tellurinate **2** in the presence of [18]crown-6. Compound **2** is

prepared by the reaction of the ditellurinic acid **1** with NaH. The direct oxidation of **1** to **3** using strong oxidants, such as  $\text{H}_2\text{O}_2$ ,  $\text{KMnO}_4$ , and  $\text{NaIO}_4$  failed.

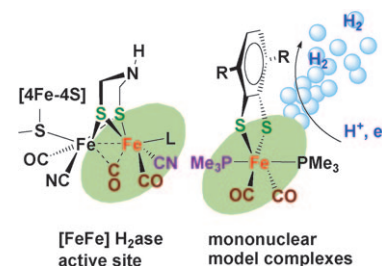
## Telluronic Acids

J. Beckmann,\* J. Bolsinger, P. Finke,  
M. Hesse ——— 8030–8032

A Well-Defined Dinuclear Telluronic Acid  $[\text{RTe}(\mu\text{-O})(\text{OH})_3]_2$



**How much iron does it take?** Mononuclear complexes  $[\text{Fe}^{\text{II}}(3,6\text{-R}_2\text{bdt})(\text{CO})_2(\text{PMe}_3)_2]$  ( $\text{bdt} = 1,2\text{-C}_6\text{H}_4(\text{S}^-)_2$ ;  $\text{R} = \text{H}, \text{Cl}$ ) can be reversibly protonated at the sulfur ligands, can catalyze the electrochemical reduction of protons, and are thus minimal functional models of the  $[\text{FeFe}]$  hydrogenases (see scheme). DFT calculations show that cleavage of an  $\text{Fe-S}$  bond leads to the generation of a free coordination site, which is crucial for the formation of hydrides that are key intermediates in the generation of hydrogen.



## Bioinorganic Chemistry

S. Kaur-Ghumaan, L. Schwartz,  
R. Lomoth,\* M. Stein,  
S. Ott\* ——— 8033–8036

Catalytic Hydrogen Evolution from Mononuclear Iron(II) Carbonyl Complexes as Minimal Functional Models of the  $[\text{FeFe}]$  Hydrogenase Active Site

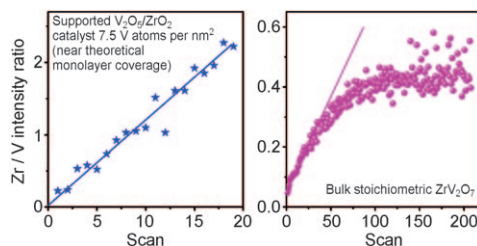


## Surface Chemistry

S. V. Merzlikin, N. N. Tolkachev,  
L. E. Briand, T. Strunskus, C. Wöll,  
I. E. Wachs, W. Grünert\* — **8037–8041**



Anomalous Surface Compositions of  
Stoichiometric Mixed Oxide Compounds



**Coated:** Surface analytical studies (including low-energy ion scattering (LEIS)) show that the outer surface of bulk, stoichiometric mixed vanadates and molybdates can be strongly enriched with

$VO_x$  or  $MoO_x$  species. Such surface reconstruction even in the calcined initial state has implications for the discussion of catalytic and other materials properties.



Supporting information is available on [www.angewandte.org](http://www.angewandte.org) (see article for access details).



A video clip is available as Supporting Information on [www.angewandte.org](http://www.angewandte.org) (see article for access details).

**Angewandte**  
WILEY  
InterScience®  
DISCOVER SOMETHING GREAT

"Hot Papers" are chosen by the Editors for their importance in a rapidly evolving field of high current interest. A preview with the graphical abstracts of these articles can be found on the *Angewandte Chemie* homepage in Wiley InterScience at [www.angewandte.org](http://www.angewandte.org).

All articles in *Angewandte Chemie* are published online several weeks ahead of print. They are found under the "EarlyView" link on the journal's homepage in Wiley InterScience.

**Angewandte**

## Service

**Spotlight on Angewandte's  
Sister Journals** — **7836–7838**

**Keywords** — **8042**

**Authors** — **8043**

**Preview** — **8045**



# Corrigendum

In this Communication (DOI: 10.1002/anie.201002870), the fourth column of Table 3, containing the reaction times *t*, was mislabeled, and wrong values for entries 6–8 were given. The correct table is shown below.

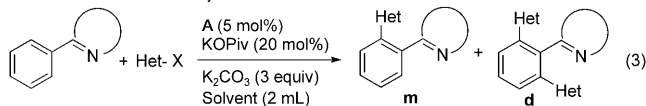
C–H Bond Functionalization in Water  
Catalyzed by Carboxylato Ruthenium(II)  
Systems

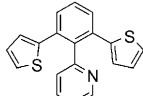
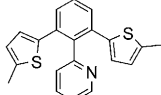
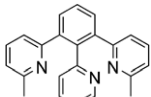
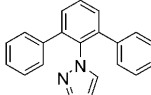
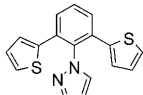
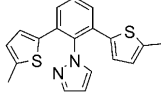
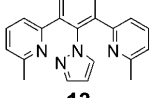
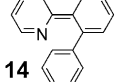
P. B. Arockiam, C. Fischmeister,  
C. Bruneau, P. H. Dixneuf\* **6629–6632**

*Angew. Chem. Int. Ed.* **2010**, *49*

DOI 10.1002/anie.201002870

**Table 3:** Functionalization of heteroarylbenzene derivatives.<sup>[a]</sup>



Entry	<i>T</i> [°C]	Solvent	<i>t</i> [h]	Conv [%]	Product	<b>m/d</b> (yield) <sup>[b]</sup>
1	100	H <sub>2</sub> O	10	100		1/99 (89)
		NMP	10	99		2/98
<b>7</b>						
2	100	H <sub>2</sub> O	10	100		1/99 (92)
		NMP	10	99		3/97
<b>8</b>						
3	100	H <sub>2</sub> O	20	100		0/100 (41)
		NMP	20	70		38/62
<b>9</b>						
4	100	H <sub>2</sub> O	2	100		0/100 (94)
	40	H <sub>2</sub> O	62	100		3/97 (90)
<b>10</b>						
5	100	H <sub>2</sub> O	10	100		4/96 (90)
<b>11</b>						
6	100	H <sub>2</sub> O	14	100		3/97 (95)
		NMP	14	95		64/36
<b>12</b>						
7	100	H <sub>2</sub> O	30	100		3/97 (48)
		NMP	30	95		17/83
<b>13</b>						
8	100	H <sub>2</sub> O	16	100		– (83)
<b>14</b>						

[a] Heteroarylbenzene (0.5 mmol), **A** (5 mol %) KOPIV (20 mol %), K<sub>2</sub>CO<sub>3</sub> (3 equiv). Het-X (1.25 mmol; see text for the identity of Het-X in each entry), 2 mL of water. [b] Yield of isolated product in parenthesis.

## Corrigendum

Scavenging Free Radicals To Preserve Enhancement and Extend Relaxation Times in NMR using Dynamic Nuclear Polarization

P. Miéville, P. Ahuja, R. Sarkar, S. Jannin,\*  
P. R. Vasos, S. Gerber-Lemaire,  
M. Mishkovsky, A. Comment,  
R. Gruetter, O. Ouari, P. Tordo,  
G. Bodenhausen 6182–6185

Angew. Chem. Int. Ed. 2010, 49

DOI 10.1002/anie.201000934

The structure in Figure 5 a in this Communication (DOI: 10.1002/anie.201000934) was printed incorrectly. The correct version of Figure 5 is shown below.

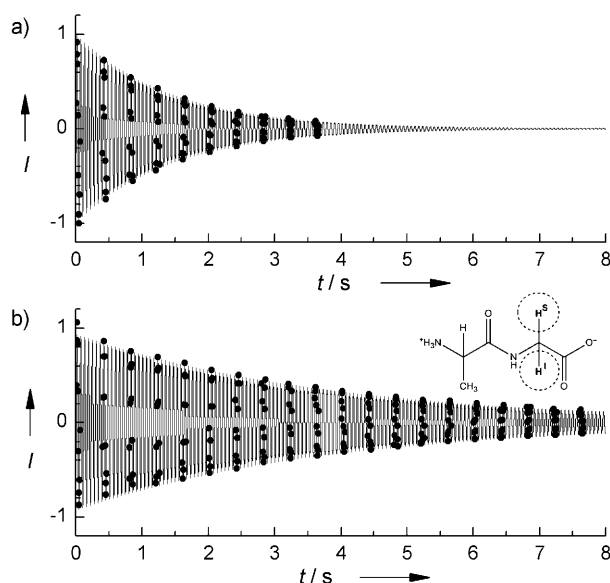
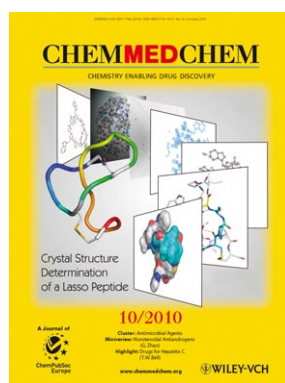


**Figure 5.** a) The decay of the long-lived coherence (LLC) involving the two protons  $H^1$  and  $H^5$  of glycine in L-Ala-Gly is affected by the presence of 2.5 mM TEMPO ( $T_{LL} = 1.43$  s). b) After addition of 30 mM sodium ascorbate, the lifetime ( $T_{LL} = 3.82$  s) is extended by a factor of 2.7. Both signals were measured at  $T = 296$  K and  $B_0 = 7.05$  T without DNP and fitted with mono-exponential decays multiplied by a sine function. The modulation arises from the scalar coupling constant  $J = -17.242$  Hz.

Check out these journals:



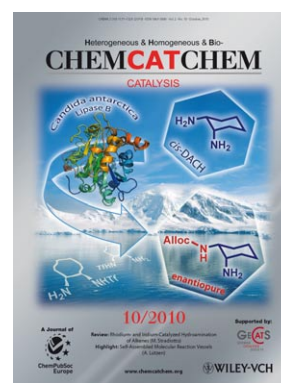
[www.chemasianj.org](http://www.chemasianj.org)



[www.chemmedchem.org](http://www.chemmedchem.org)



[www.chemsuschem.org](http://www.chemsuschem.org)



[www.chemcatchem.org](http://www.chemcatchem.org)